Malays. J. Bioeng. Technol. Vol. 2, No. 2, (2025): 60-78
https://doi.org/10.70464/mjbet.v2i2.1602

MALAYSIAN JOURNAL OF BIOENGINEERING AND TECHNOLOGY

MJBeT Malaysian Journal of Bioengineering and Technology

Comparative Investigation on the Optimisation of Hydrogel Derived from Cellulose of Banana Stem (Musa x paradisiaca), Cellulose and Carboxymethylcellulose (CMC) Crosslinked Using Citric Acid

Wong Yee Ching*, Kee Shu Huey, Anussha A/P Shankar

Bioproduct and Bioprocessing Technology Research Group, Faculty of Bioengineering and Technology, Universiti Malaysia Kelantan, Jeli Campus, Jeli 17600, Kelantan, Malaysia

**Corresponding author: yeeching@umk.edu.my*

ARTICLE INFO

Received:25 May 2025
Accepted:20 June 2025
Online:30 June 2025
eISSN: 3036-017X

ABSTRACT

This study explores citric acid as a viable crosslinking agent for the development of hydrogels derived from banana stem cellulose, commercial cellulose, and carboxymethylcellulose (CMC). It addresses the environmental impact of banana stem waste by advocating for sustainable cellulose extraction to reduce pollution from open burning. The alkaline-based extraction method successfully transforms 43% of banana stem powder, with critical considerations for Sodium hydroxide (NaOH)/Sodium hypochlorite (NaOCl) concentrations, extraction temperature, and lignin removal duration to optimise cellulose yield. Microscopy analysis confirms the fibrous nature of banana stem cellulose, distinguishing it from non-fibrous CMC. Its fibrous content influences dissolution in 8% NaOH and 12% urea, as the treatment helps break down the rigid fibres in the banana stem, making the cellulose easier to dissolve for subsequent use. Its higher fibrous content influences dissolution in 8% NaOH and 12% urea, impacting hydrogel properties and highlighting the need for precise dissolution conditions. The concentration of citric acid plays a pivotal role in the crosslinking process, influencing hydrogel characteristics. Hydrogels prepared with 40% citric acid show efficient crosslinking, a crucial factor for desirable properties. Comparative analyses employing FTIR Spectroscopy and SEM imaging distinguish Banana Stem Cellulose Hydrogel (BSCH), Cellulose Hydrogel (CH), and Carboxymethylcellulose Hydrogel (CMCH). The FTIR spectra reveal distinct peaks associated with hydroxyl groups, confirming the hydrophilic nature of the hydrogels. SEM images showcase BSCH's fibrous and porous structure, emphasising its potential in applications like wound dressings. Antibacterial tests indicate BSCH's enhanced effectiveness against *Escherichia coli*, attributed to citric acid inclusion. Adsorption studies demonstrate BSCH's superior efficiency in removing methylene blue dye. Biodegradation investigations reveal BSCH's controlled degradation (91%), outperforming CH (89%) and CMCH (100%), making it a promising material for wound care and environmental remediation.

Keywords: Banana Stem Cellulose Hydrogel; Cellulose Hydrogel; Carboxymethylcellulose Hydrogel; Citric Acid

1. Introduction

Hydrogels are crosslinked polymer networks renowned for their high water retention capacity and stability, making them ideal for diverse applications such as wound healing, agriculture, and drug delivery. Cellulose, particularly that derived from agricultural waste such as banana stems, is a biodegradable, abundant, and renewable resource suited for hydrogel synthesis. In Malaysia, banana plantations generate large amounts of post-harvest biomass, especially banana stems, raising environmental concerns due to open burning and poor waste management. This study emphasises the sustainable extraction and utilisation of banana stem cellulose for hydrogel formulation. By leveraging the hydrophilic and modifiable nature of cellulose and carboxymethylcellulose (CMC), and using citric acid as a green crosslinker, this research explores novel, eco-friendly hydrogels for biomedical and environmental use.

Current wound dressing practices are inefficient, leading to material waste due to poor application, contamination, and improper sizing. This is worsened by inadequate training among healthcare professionals, highlighting the need for improved education and standardised application techniques. Meanwhile, banana plantations generate significant waste, which accounts for up to 60% of the plant biomass, which is often burned, contributing to environmental pollution and greenhouse gas emissions. Furthermore, existing hydrogel synthesis methods often rely on toxic chemicals, posing potential health risks due to residual solvents or monomers. These issues highlight the dual need to optimise waste biomass utilisation and develop safer, more sustainable hydrogel systems.

This study contributes to environmental sustainability and biomaterial science by demonstrating the value of banana stem waste as a cellulose source for hydrogel production. Using citric acid as a crosslinking agent underscores the eco-friendly approach in hydrogel formulation, enhancing biocompatibility and water absorption properties. Comparative analysis of hydrogels derived from banana stem cellulose, commercial cellulose, and CMC provides key insights into their structural, chemical, and functional differences, revealing their suitability for specific biomedical or environmental applications. By addressing material performance and biodegradability, the study helps bridge knowledge gaps in green hydrogel technologies and supports future advancements in wound care and environmental remediation.

2. Materials and Methods

2.1 Materials and Chemicals

The materials that were used in this study are Banana Stems from the species Musa x paradisiaca, which were harvested from the Jeli region of University Malaysia Kelantan (UMK). 5 kg of banana stems were used as the primary raw material for the project. The stems were selected and harvested from local banana plants in the Agro Park UMK Jeli.

In this study, the chemicals used were Sodium Hydroxide (NaOH, ≥98%, HmbG), Sodium Hypochlorite (NaOCl, 5-6% solution, Systerm), Cellulose (microcrystalline, R&M), Carboxymethyl Cellulose (CMC, pharmaceutical grade, R&M), Urea (≥99%, HmbG), and Citric Acid (CA, anhydrous, ≥99%, HmbG).

2.2 Methods for the Formation of Banana Stem Cellulose and Cellulose-Based Hydrogel

2.2.1 Collect and prepare the banana stem

Banana stems were collected from UMK Agro Park, washed, sliced, and oven-dried at 60°C for 24 hours (Fig. 1). The dried stems were then ground to a 250-mesh using a blender and stored in zipper bags for later use [1].

eISSN Number: 3036-017X

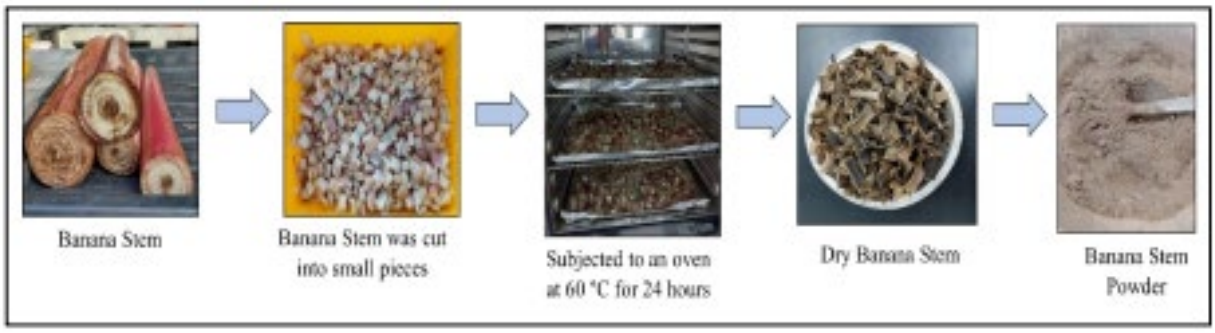

Fig. 1: Procedure for the preparation of Banana Stem Powder

2.2.2 Extraction of cellulose from banana stem

Cellulose was extracted from banana stem following the method by Susi et al. [2]. Banana stem powder was treated with 8% NaOH (1:20 w/v) at 100°C for 3.5 hours to remove lignin and hemicellulose, producing a dark slurry. The mixture was filtered and rinsed with distilled water, then bleached with 5% NaOCl at 30°C for 3 hours. After thorough washing to remove any residual odour, the purified cellulose was dried at 60°C in a cabinet dryer.

2.2.2.1 Lignin removal

To initiate the process, 25 grams of banana stem powder were introduced into a 1000 ml beaker along with 500 ml of 8% (w/v) NaOH solution. The mixture was subjected to heating on a hot plate at 100°C for a duration of 3.5 hours. The purpose of this step was to eliminate the lignin content present in the banana stem. Through this thermal treatment, the non-cellulosic components broke down and dissolved in the solution, leaving behind purified cellulose.

2.2.2.2 Bleaching process

To remove residual lignin and hemicellulose, the washed cellulose was bleached with a 5% NaOCl solution [3][4]. About 500 ml of the bleach was added to the cellulose in a 1000 ml beaker and stirred at 30°C for 3 hours. NaOCl was selected for its strong oxidising properties to break down lignin and hemicellulose. After bleaching, the cellulose was thoroughly washed with distilled water and vacuum filtered to obtain purified, white cellulose powder.

2.2.2.3 Dissolve banana stem cellulose and cellulose

To dissolve banana stem cellulose or cellulose, 0.8 g NaOH and 1.2 g urea were dissolved in 10ml of distilled water. Then, 0.5 g of cellulose was added and stirred vigorously in an ice bath for 1 hour. The NaOH-urea mixture acted synergistically to break down the cellulose structure, making it water-soluble [5].

2.2.2.4 Forming of banana stem cellulose or cellulose-based hydrogel using citric acid

Banana Stem Cellulose or Cellulose was dissolved in solvent, then citric acid (CA) at 10, 20, 30, or 40% (m/m), where (m/m) refers to mass of citric acid per mass of total solution was added and stirred for 18 minutes at 70°C (10 ml solution). These temperatures and duration were selected based on previous studies showing that moderate heat facilitates effective ester bond formation between citric acid and the hydroxyl groups on cellulose without degrading the polymer [2]. Such crosslinking improves hydrogel properties while maintaining structural integrity. Stirring rate affected solvent evaporation and hydrogel texture, requiring careful control for optimal formation. CA acted as a crosslinker, and the mixture underwent two freeze-thaw cycles (−20°C for 3 hours, then room temperature for 3 hours) to promote gelation and hydrogel formation [5].

2.3 Methods for the formation of Carboxymethylcellulose (CMC) Hydrogels

The CMC powder was mixed with distilled water (20% CMC) to form a paste, shaped in a mould and pressed to remove air bubbles. At this stage, the CMC chains remained uncross-linked. The moulded paste was then soaked in citric acid (6 mol/L to saturation) for 12 hours, promoting hydrogen bonding and hydrogel formation. Finally, the hydrogel was immersed in distilled water for two days to stabilise and optimise its properties [6].

eISSN Number: 3036-017X

2.4 Hydrogel Characterisation

2.4.1 Fourier transform infrared (FTIR) spectroscopy

FTIR analysis performed using a PerkinElmer Spectrum Two instrument, scanning from 4000 to 400 cm^{-1} with 4 cm^{-1} resolution and 32 scans per sample. The test is to identify functional groups and molecular changes in Banana Stem Cellulose, Cellulose, and Carboxymethylcellulose powders and their hydrogels. Special attention was given to peak shifts caused by citric acid crosslinking, revealing structural modifications during hydrogel formation.

2.4.2 Scanning electron microscopy (SEM)

SEM imaging was used to examine the microstructure of the hydrogels. Samples were freeze-dried, mounted, and observed under high vacuum at various magnifications (500x to 2000x). This provided detailed information on surface morphology, pore size, distribution, porosity, and fibre orientation.

2.4.3 Antibacterial testing

Nutrient agar plates were inoculated with 18–24-hour cultures of *Escherichia coli*. Sterile 3 mm filter paper discs were placed on the agar surface, with chloramphenicol discs (3.5 mg each) serving as positive controls. Three hydrogel types (Banana Stem Cellulose, Cellulose, and Carboxymethylcellulose) were applied to separate discs.

All plates were incubated at 37°C for 18–24 hours. Zones of inhibition were measured the next day to assess the antibacterial efficacy of each hydrogel, based on the size of the clear area surrounding the discs.

2.4.4 Adsorption of methylene blue dye test

Hydrogels (Banana Stem Cellulose, Cellulose, and Carboxymethylcellulose) were freeze-dried and tested for methylene blue dye adsorption. A series of methylene blue solutions (25–200 mg/L) was prepared from a 500 mg/L stock. Approximately 0.05 g of each hydrogel was added to 5 ml of dye solution in 10 ml volumetric flasks and incubated at room temperature for 24 hours. Equation 3.1 was used to compute the equilibrium quantity of adsorbed dye (QE, mg/g).

$$QE = \frac{(Ci - CE)}{m} \times V \quad (1)$$

where Ci and CE are the initial and final dye concentrations (mg/L), V is the volume (L), and m is the hydrogel mass (g).

2.4.5 Biodegradation test

Hydrogels were buried in soil to monitor degradation through weight loss and morphological changes over 28 days, with measurements taken every 7 days. This evaluated the environmental breakdown and microbial interaction with the hydrogels over time.

3. Results and Discussion

3.1 Extraction of Banana Stem Cellulose Fibre by using Alkaline-Based Methods

NaOH acts as a hydrolysis agent in cellulose extraction by breaking hydrogen bonds between hemicellulose and cellulose and degrading lignin due to its strong alkalinity [7]. Lignin, a hydrophobic, cross-linked polymer, binds cellulose and hemicellulose in plant cell walls and aids water transport [8]. NaOH effectively dissolves lignin, facilitating cellulose isolation from lignocellulosic biomass.

eISSN Number: 3036-017X

3.1.1 Delignification of banana stem powder

An 8% NaOH solution was used to delignify banana stem powder [2] [9], which identified this concentration as optimal for effective lignin removal without degrading cellulose. Lower concentrations risk incomplete delignification, while higher levels may damage cellulose quality.

The solvent becomes dark brown after heating at 100°C for 3.5 hours, indicating increased concentration due to lignin dissolution as shown in Fig. 2. This colour change is due to NaOH breakdown of lignin during the extraction process. The solvent's colour becomes dull, which reflects successful lignin removal. The colour shift may be more evident if the banana stem has high lignin content [10]. Furthermore, changes in solvent colour during the extraction process can be used as a qualitative indication of the chemical processes and the effectiveness. Monitoring these changes may aid in optimising process conditions for extracting desired components from the banana stem.

Fig. 2: Banana Stem powder dissolved with NaOH

NaOH treatment of banana stem powder increases the solubility of lignin through alkaline hydrolysis, aiding lignin removal. Moreover, in organic chemistry, the alkaline hydrolysis is a form of nucleophilic substitution process in which the attacking nucleophile is a hydroxide ion. Therefore, the reaction products are mainly water-soluble salts and the matching phenol, which are less likely to be harmful to the environment due to their use of less energy than traditional cremation, making it a more ecologically friendly alternative compared with other extraction methods [11]. The reaction can be represented in Fig. 3.

NaOH breaks ester bonds in lignin, dissolving it into lignin derivatives and turning the solution dark brown. After 3.5 hours, the mixture is vacuum filtered with distilled water until neutral. Longer immersion and higher NaOH concentration slow filtration and reduce cellulose yield, requiring large volumes of water to aid filtration and prevent cellulose degradation.

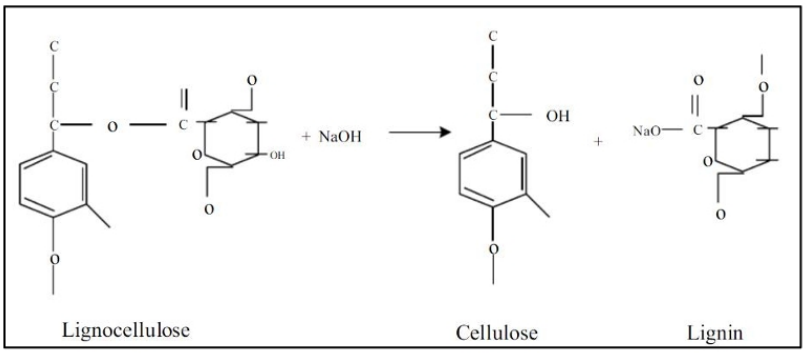

Fig. 3: The mechanism of interaction between lignocellulose and NaOH

eISSN Number: 3036-017X

3.1.2 Optimal parameters for the pre-treatment bleaching process

The bleaching process aims to remove impurities such as lignin, hemicellulose, extractives, and colourants from banana stem cellulose. This enhances purity, improves quality, and produces a cleaner, whiter cellulose suitable for applications requiring a colourless final product (Fig. 4).

Fig. 4: Bleaching treatment by using NaOCl

To remove colour-causing impurities and enhance the brightness of banana stem cellulose, a 5% sodium hypochlorite (NaOCl) solution was used during bleaching. NaOCl, containing strong oxidising hypochlorite ions, breaks ether bonds in lignin, effectively decolourising the cellulose. The solution, prepared from a 10% chlorine stock, was heated to 30°C and applied for 3 hours to maximise whitening efficiency.

3.1.3 Yield of banana stem cellulose

To calculate the yield of Banana Stem Cellulose after the alkaline treatment, which involves using 8% NaOH and a bleaching process, which involves using 5% NaOCl to extract the cellulose from the banana stem. The cellulose content was calculated using Equation 2:

$$Yield\ (\%) = \frac{Weight\ of\ Banana\ Stem\ Cellulose}{Weight\ of\ Initial\ of\ Banana\ Stem\ Powder} \times 100 \quad (2)$$

$$= \frac{8.778\ grams}{20.003\ grams} \times 100$$

$$= 43.883$$

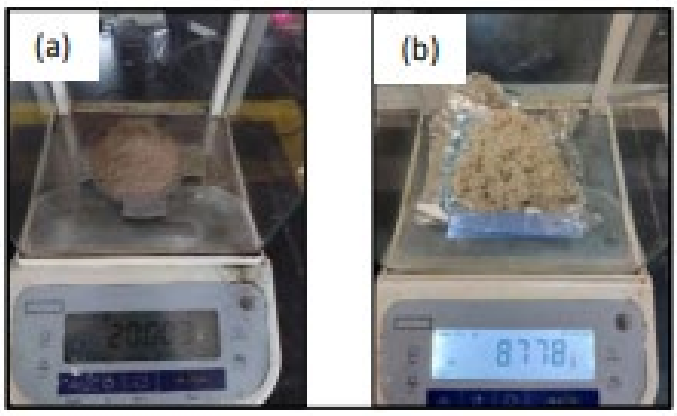

Fig. 5: Weight before and after the alkaline treatment process (a) Initial weight of Banana Stem Powder, (b) Final weight of Banana Stem Cellulose Powder

eISSN Number: 3036-017X

The yield (%) is calculated by dividing the weight of extracted Banana Stem Cellulose (Fig. 5) by the original Banana Stem Powder weight, then multiplying by 100. This indicates how efficiently cellulose was extracted from the raw material.

A 43% yield of cellulose was achieved from the initial banana stem powder. This result aligns well with findings by Susi et al., who reported cellulose yields ranging from 40% to 45% using similar alkali treatment conditions [2]. The consistency between these results reinforces the effectiveness of using 8% NaOH for lignin removal while preserving the structural integrity of cellulose. Yield varied with extraction conditions like NaOH/NaOCl concentration, temperature, and lignin removal time. High NaOH concentration and high temperatures risk cellulose degradation, while too short or too long lignin removal affects purity or causes breakdown. Optimal conditions are essential to balance yield and cellulose quality.

3.2 Morphological Characterisation of Banana Stem Cellulose, Cellulose and Carboxymethyl Cellulose (CMC) through Microscopy

In the observation of banana stem cellulose in Fig. 6 under 4x and 10x magnification, had reveals the different traits. At a moderate 4x magnification, the cellulose forms a thick, interwoven network fibres with random orientation, at this magnification. Ironically, because of its intrinsic poor resolution, this level of Fig. 6 presents Optical Microscopy and SEM micrographs of banana stem as a cellulose source, displaying images at various magnifications: (a) 4× and (b) 10× using an optical microscope, and (c) 500× and (d) 750× using SEM. Notably, at 36× magnification, detecting individual fibres becomes challenging. At 10x, fibres appear clearer with visible striations, branching, and kinks, revealing more structural details. This progressive magnification enhances understanding of the complex fibre network in banana stem cellulose.

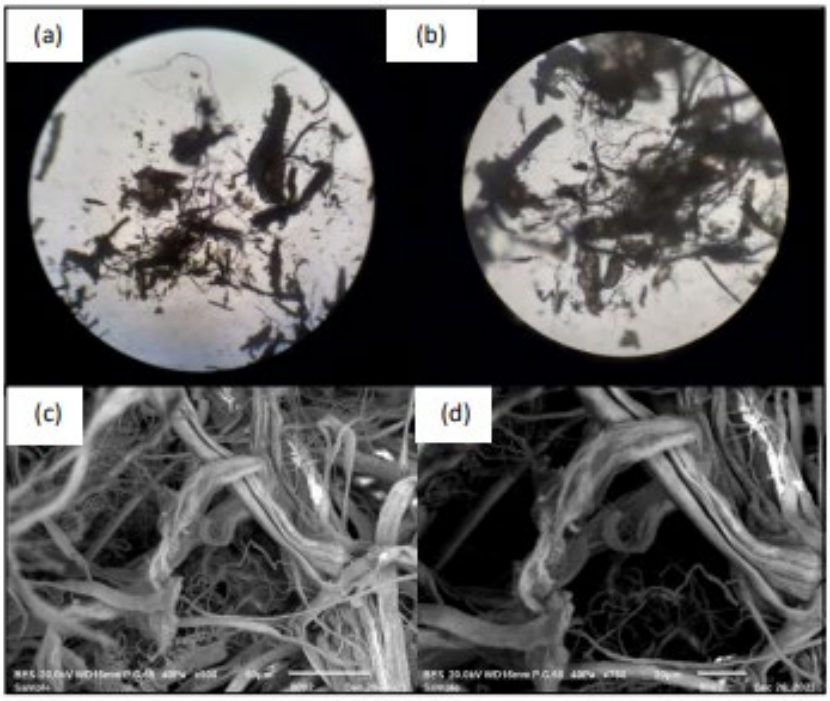

Fig. 6: Optical Microscopy and SEM micrographs of Banana Stem as a cellulose source. (a) 4x magnification from optical microscope (b) 10x magnification from optical microscope (c) 500x magnification from SEM (d) 750x magnification from SEM

SEM images at 500x and 750x reveal detailed cellulose fibres with rough surfaces featuring pits, grooves, and ridges. The fibrous network and fibre orientations become clearer at higher magnification, showing striations and internal hollows. Optical microscopy confirms effective extraction of banana stem cellulose fibres with varied rough textures. These structural details highlight the fibres' potential for applications needing lightweight composites, large surface area, and specialised internal features.

eISSN Number: 3036-017X

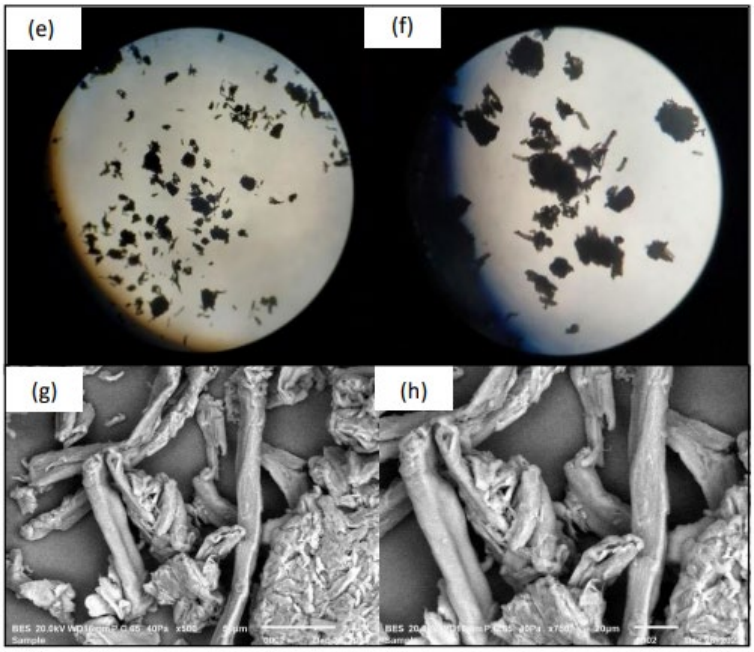

Fig. 7: Optical Microscopy and SEM micrographs of Cellulose powder. (a) 4x magnification from optical microscope (b) 10x magnification from optical microscope (c) 500x magnification from SEM (d) 750x magnification from SEM

Fig. 7 shows cellulose under optical microscopy at 4x and 10x magnification. At 4x, cellulose appears thick and mostly amorphous, with no clear fibre structure, indicating a non-fibrous, clumped form. At 10x, slight striations and smoother particle edges are visible, but individual fibres remain unclear. This suggests that commercial cellulose is likely processed into a microcrystalline form, altering its natural fibrous structure.

SEM at 500x shows cellulose powder with an uneven, fractured, and rough surface featuring sharp edges, platelet-like shapes, and particle agglomerates, confirming its non-fibrous, microcrystalline nature. At 750x, the broken structure with visible pores, cavities, and fissures becomes clearer, highlighting a rougher, more complex surface and defined particle sizes. These features indicate processed cellulose, suitable for applications requiring high surface area or controlled particle size.

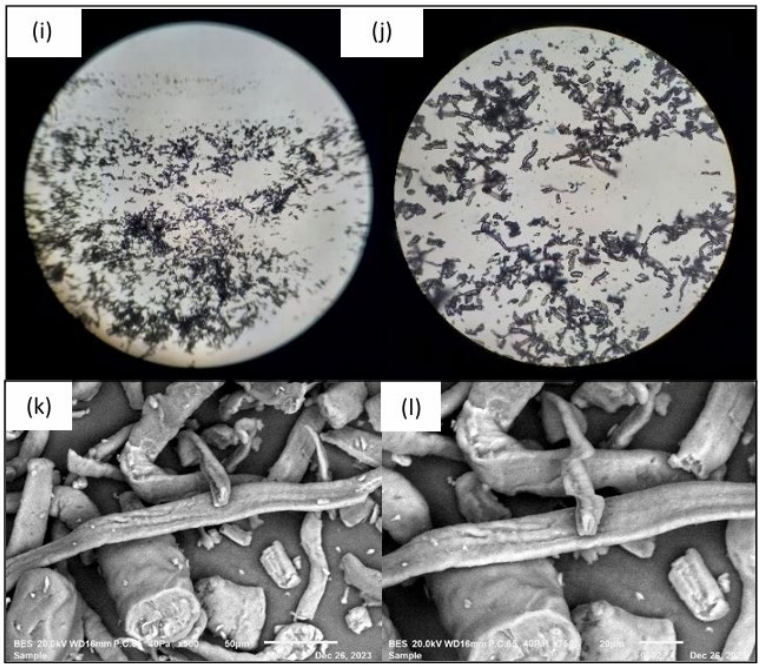

Fig. 8: Optical Microscopy and SEM micrographs of CMC. (a) 4x magnification from optical microscope (b) 10x magnification from optical microscope (c) 500x magnification from SEM (d) 750x magnification from SEM

eISSN Number: 3036-017X

Fig. 8 shows CMC powder under optical microscopy at 4x (i) and 10x (j) magnifications, and SEM at 500x (k) and 750x (l). At 4x (i), CMC appears as thick, irregular particles without fibrous structure, with some collapse patterns, but hard to measure due to agglomeration. At 10x (j), the particles remain non-fibrous with finer granular details, though individual sizes are still unclear. This indicates that chemical modification (carboxymethylation) alters the original cellulose fibre structure, resulting in a non-fibrous, particle-like form.

Image (k) at 500x SEM shows CMC powder with an uneven, fractured structure featuring sharp edges, platelet-like forms, and rough, possibly porous surfaces, confirming its non-fibrous nature due to carboxymethylation. This structure supports applications like thickening and binding. At 750x magnification (l), surface details are clearer, revealing pores, cavities, and internal fissures, with particle sizes under 1 micron. This image reinforces the modified, non-fibrous nature of CMC, aligning with literature [1,6,10] that highlights its enhanced water-holding capacity, biodegradability, and reactivity compared to natural cellulose. These characteristics further support its suitability for various applications requiring tailored material properties.

Optical microscopy (OM) and SEM analyses reveal distinct differences among banana stem cellulose, standard cellulose, and carboxymethylcellulose (CMC) powders. Banana stem cellulose shows a natural fibrous network, while standard cellulose and CMC appear non-fibrous. All have rough surfaces, but CMC is notably rougher and more porous due to carboxymethylation. SEM shows common features like pits and grooves in all samples, with CMC displaying additional fractures and voids, indicating structural disruption. Overall, banana stem cellulose retains fibrous strength, standard cellulose suits non-fibrous uses, and CMC's altered morphology suits thickening, gelling, and binding applications.

3.3 Comparing and Optimising the Production of Banana Stem Cellulose Hydrogel, Cellulose Hydrogel, and Carboxymethyl Cellulose Hydrogel Synthesis

Fig. 9 shows hydrogels made from banana stem cellulose, generic cellulose, and carboxymethyl cellulose (CMC), each with distinct appearances. Image (a) shows the banana stem cellulose hydrogel, which looks slightly cloudy brown with a smooth texture, indicating successful crosslinking. Fig. 9(b) presents the cellulose hydrogel, which is more transparent and appears softer than Fig. 9(a), reflecting typical cellulose hydrogel traits. Fig. 9(c) depicts the CMC hydrogel, which is translucent like the others but more elastic due to carboxymethyl groups in its structure. These visual differences highlight the unique properties of each hydrogel type based on their preparation.

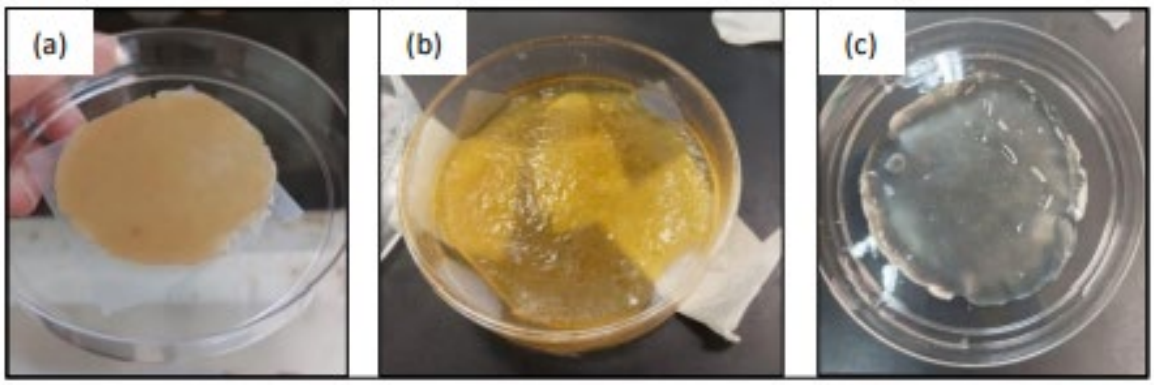

Fig. 9: The synthesis of hydrogel involves the preparation of cellulose from a distinct variety, employing citric acid as the crosslinking agent. (a) Banana Stem Cellulose Hydrogel (b) Cellulose Hydrogel (c) CMC Hydrogel

3.3.1 Optimising the dissolution of untreated banana stem cellulose powder and untreated cellulose powder

Fig. 10 illustrates the discernible physical transformation occurring before and after the dissolution process of untreated banana stem cellulose powder and commercial cellulose powder. The labelled segments (a) and (b) depict the initial states of banana stem cellulose powder and commercial cellulose powder, respectively, undergoing dissolution with 8% NaOH and 12% urea. Conversely, labelled (c) and (d) represent the subsequent states after the banana stem cellulose powder, showing enhanced swelling and structural loosening, which prepares the cellulose for subsequent gel formation during freeze-thaw cycling at -20°C for a duration of 24 hours.

eISSN Number: 3036-017X

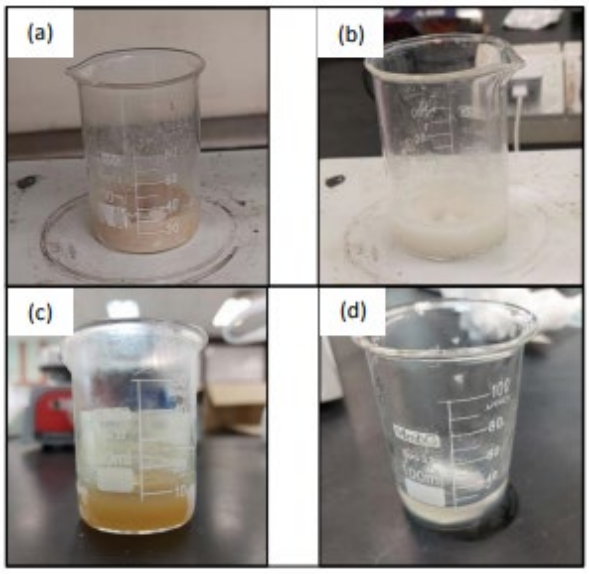

Fig. 10: Texture observed pre- and post-dissolution of cellulose (a) before banana stem cellulose dissolves in the solvent, (b) before cellulose dissolves in the solvent, (c) untreated banana stem cellulose, (d) untreated cellulose

The untreated banana stem cellulose solution appears brownish, unlike the clear, transparent solution of untreated commercial cellulose. This difference is due to the less thorough bleaching of banana stem cellulose, resulting in lower purity compared to the highly purified commercial cellulose. The contrast highlights differences in extraction and purity between the samples.

3.3.2 Optimising citric acid concentrations for banana stem cellulose and cellulose in the synthesis of hydrogels

The concentration of citric acid is an essential factor in determining the characteristics of the resulting hydrogel during the crosslinking process. Inadequate citric acid concentrations can result in weak gels with reduced swelling ability, whilst excessive amounts might inhibit gel formation or produce too brittle hydrogels. Obtaining the correct concentration requires thorough testing, depending on the exact cellulose variety used

As shown in Fig. 11, the unsuccessful formation of the hydrogel was labelled as a, b and c, showing the different percentages of the formation of the banana stem cellulose hydrogel by using 10%, 20% and 30% of the citric acid for the formation of the hydrogel, respectively. However, labelled d, e and f show that the different percentages of the formation of the cellulose hydrogel by using 10%, 20% and 30% respectively.

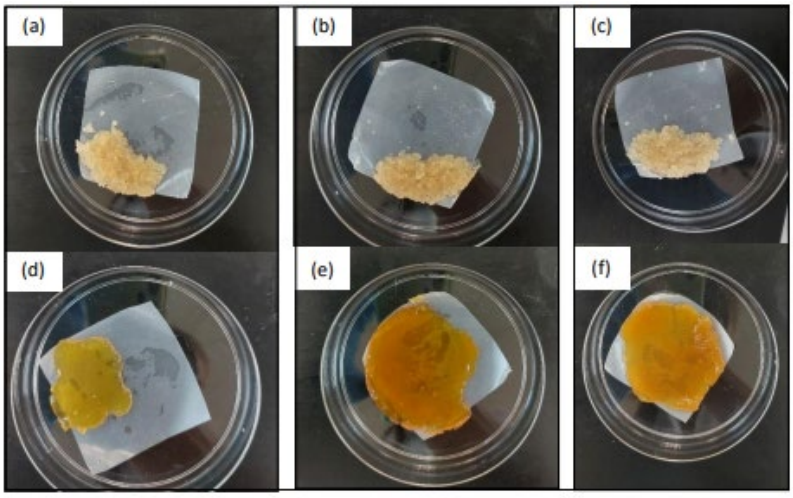

Fig. 11: Optimal parameters for the formation of hydrogel through the utilization of citric acid. (a) BSC-CA10% (b) BSC-CA20% (c) BSC-CA30% (d) CelluloseCA10% (e) Cellulose-CA20% (f) Cellulose-CA30%

eISSN Number: 3036-017X

3.4 Comparative Analysis of Banana Stem Cellulose Hydrogel, Cellulose Hydrogel, and Carboxymethylcellulose Hydrogels

3.4.1 Fourier transform infrared (FTIR) spectroscopy

Fig. 12 shows FTIR spectra of three hydrogels: Banana Stem Cellulose (BSC_H), Cellulose (C_H), and Carboxymethylcellulose (CMC_H). All have strong -OH stretching peaks around 3338–3344 cm^{-1}. BSC_H and C_H show sharp carbonyl (C=O) peaks at about 1625 cm^{-1}, while CMC_H has a moderate peak at 1636 cm^{-1}. These peaks reflect the polysaccharide structure with glucose units linked by β-1,4-glycosidic bonds.

FTIR analysis also shows differences in the methylene (CH2) group: BSC_H and C_H have strong, sharp peaks at about 1371 cm^{-1}, while CMC_H shows a much weaker peak. Additionally, strong C-O stretching vibrations of primary ethers and alcohols appear at 1020.04 cm^{-1}, 1020.20 cm^{-1}, and 1058.44 cm^{-1} for BSC_H, C_H, and CMC_H, respectively.

Fig. 13 shows FTIR spectra of Banana Stem Powder (BSC_P), Cellulose Powder (C_P), and Carboxymethyl Cellulose Powder (CMC_P). All powders have two main absorption regions: 950-1150 cm^{-1} and 3000-3500 cm^{-1}, showing similarities. BSC_P and C_P have broad -OH peaks at 3335.34 cm^{-1} and 3327.65 cm^{-1}, while CMC_P's -OH peak is broader and lower at 3231.05 cm^{-1}, indicating slight structural differences. Methylene (-CH2-) peaks are moderately intense for BSC_P (2900.97 cm^{-1}) and C_P (2894.83 cm^{-1}), but weaker for CMC_P (2880.50 cm^{-1}). At ~1418 cm^{-1}, BSC_P and C_P show weak-moderate peaks, while CMC_P has a stronger peak. All three show strong ether (C–O–C) bands near 1020 cm^{-1}, confirming similar chemical bonds.

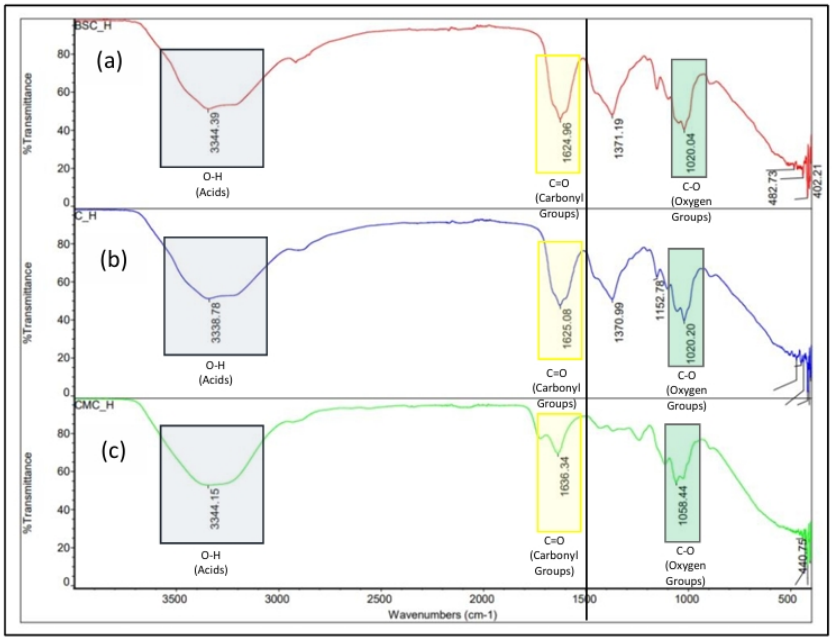

Fig. 12: Fourier transform infrared spectroscopy (FTIR) spectra: (a) BSC Hydrogel, (b) Cellulose Hydrogel, (c) CMC Hydrogel

Fig. 14 presents FTIR spectra of three untreated hydrogels: Banana Stem Cellulose (UN_BSC), Cellulose (UN_C), and Carboxymethylcellulose (UN_CMC). All three show a strong -OH stretching peak near 3300 cm^{-1}: 3343.12 cm^{-1} (UN_BSC), 3335.44 cm^{-1} (UN_C), and 3317.18 cm^{-1} (UN_CMC), indicating hydroxyl groups from the polysaccharide chains. The carbonyl (C=O) peaks appear around 1628–1636 cm^{-1}: 1628.30 cm^{-1} (UN_BSC), 1629.31 cm^{-1} (UN_C), and 1636.07 cm^{-1} (UN_CMC), with slight intensity differences. A C–O stretching peak at 1019.95 cm^{-1} is only visible in UN_C, suggesting a structural difference in the cellulose backbone. These FTIR results highlight chemical variations between the hydrogels.

eISSN Number: 3036-017X

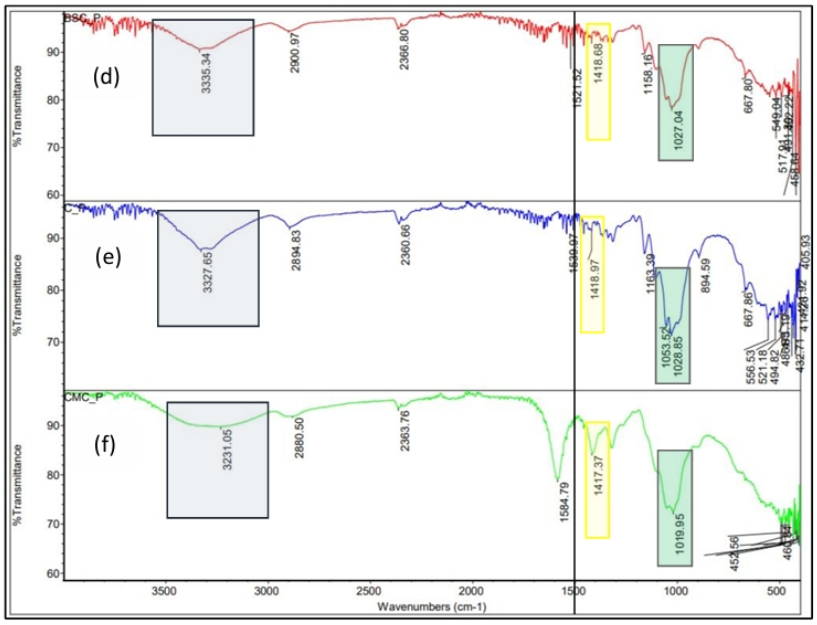

Fig. 13: Fourier transform infrared spectroscopy (FTIR) spectra: (d) BSC Powder, (e) Cellulose Powder, (f) CMC Powder

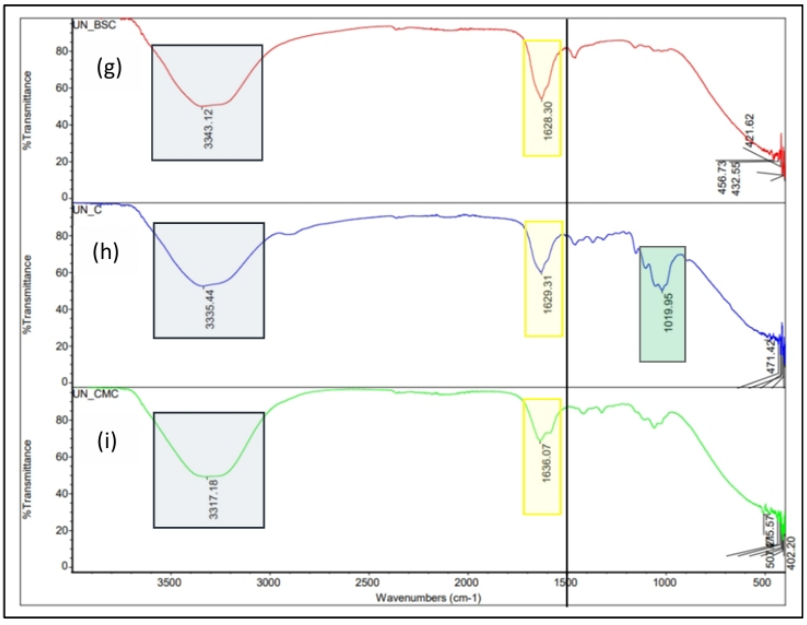

Fig. 14: Fourier transform infrared spectroscopy (FTIR) spectra: (g) Untreated BSC (h) Untreated Cellulose (i) Untreated CMC Powder

3.4.2 Scanning electron microscope (SEM) analysis of banana stem cellulose-based hydrogels

Fig. 15 shows SEM images of banana stem cellulose hydrogel at different magnifications. Image (a) at 500x reveals a relatively smooth surface with holes, likely caused by the removal of lignin and other non-cellulosic materials. Image (b) at 1000x shows a complex, interconnected network of cellulose fibres that form the hydrogel's structure. At 1500x magnification, image (c) highlights the rough surface of the fibres with visible striations due to the crystalline nature of cellulose. Finally, image (d) at 2000x displays individual cellulose microfibrils that make up the fibres. Overall, these SEM images demonstrate that the banana stem cellulose hydrogel is a porous material with a linked fibre network, where its strength and unique properties stem from its crystalline structure and rough fibre surface, making it suitable for various applications.

Fig. 16 shows SEM micrographs of cellulose-based hydrogels at four different magnifications to highlight their structural features. At 500× magnification (e), the hydrogel surface looks relatively smooth with noticeable pores,

eISSN Number: 3036-017X

indicating gaps between cellulose fibres. The slight asymmetry in the structure may be due to additional components or additives present in the commercial cellulose product. At 1000× magnification (f), the network of cellulose fibres becomes clearer, revealing intricately interwoven strands that form the backbone of the hydrogel matrix. These fibres display varied textures, from rough to smooth, depending on the processing techniques used. At 1500× magnification (h), striations along the fibre surfaces are visible, reflecting the crystalline nature of cellulose. The increased density of the fibre network in this image suggests the crosslinking effect of citric acid. Finally, at 2000× magnification (i), individual cellulose microfibrils with diameters from 2 to 5 nm are observed. These microfibrils are more organised and aligned, indicating the structural influence of citric acid crosslinking compared to other agents.

Fig. 17 shows SEM micrographs of carboxymethylcellulose (CMC)-based hydrogels at different magnifications. At 500× magnification (i), the hydrogel surface looks smooth with visible pores, which likely indicate gaps between CMC polymer chains. The slight asymmetry in the structure may result from crosslinking effects or additional ingredients used during hydrogel formation. At 1000× magnification (j), a clearer image of the CMC network reveals interwoven chains forming the hydrogel matrix. The smoother texture of these chains, compared to regular cellulose, is due to the presence of carboxymethyl groups. At 1500× magnification (k), finer structural details such as increased density at crosslinking points and striations become visible, indicating partial crystallinity within the CMC structure. At the highest magnification of 2000× (l), elongated, linear CMC chains are observable with attached carboxymethyl groups. This highlights the effect of citric acid crosslinking in forming an organised and stable hydrogel network.

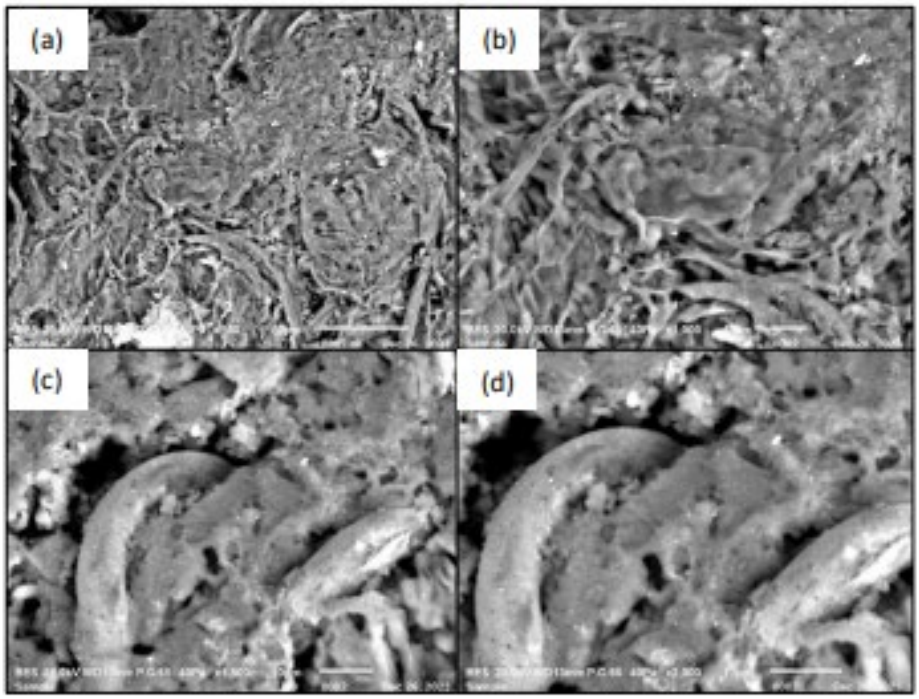

Fig. 15: SEM micrographs depicting hydrogels prepared from banana stem as the source of cellulose

eISSN Number: 3036-017X

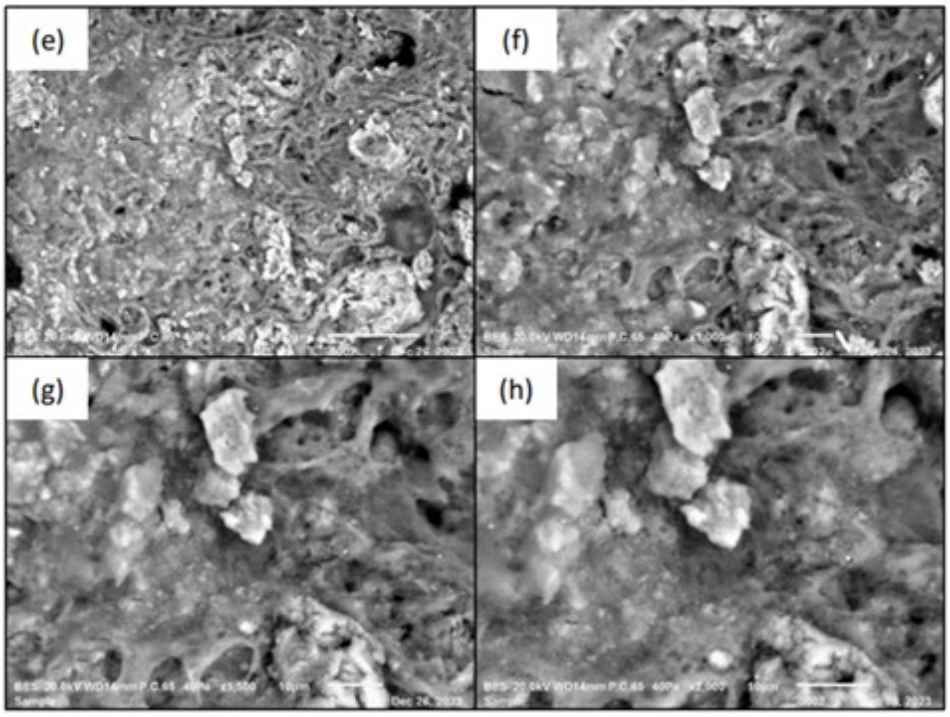

Fig. 16: SEM micrographs depicting hydrogels prepared from cellulose

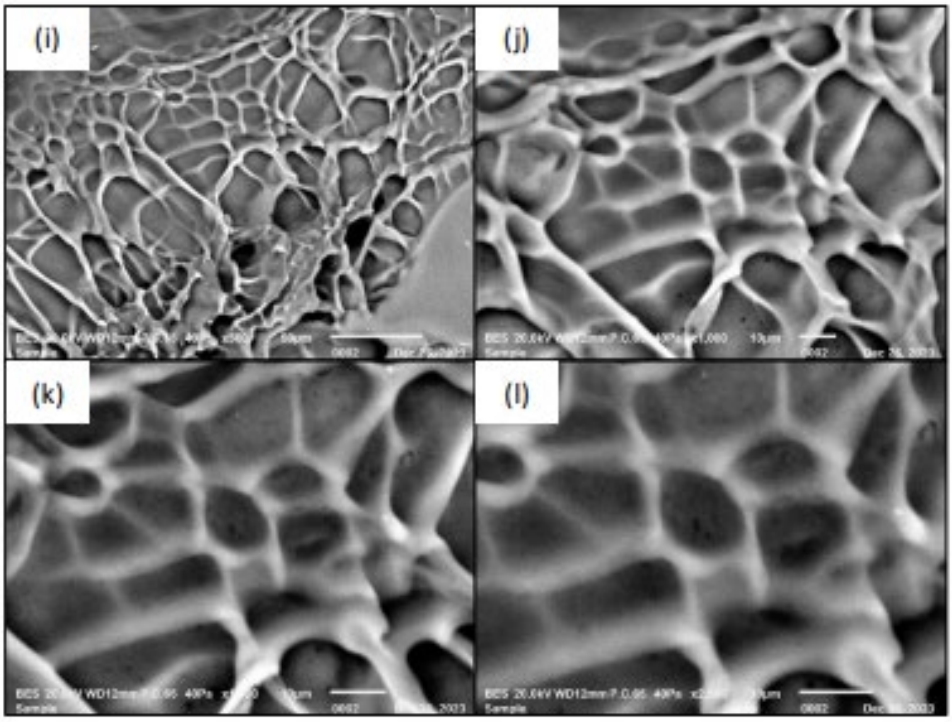

Fig. 17: SEM micrographs depicting hydrogels prepared from CMC

3.4.3 Antibacterial test

Escherichia coli (E. coli), a common Gram-negative bacterium with a unique outer membrane, was chosen for hydrogel antibacterial testing due to its relevance and ease of lab cultivation. Chloramphenicol, a broad-spectrum antibiotic, was used as a positive control in *E. coli* antibacterial tests (a, b, c), providing a benchmark to verify the test method and assess the hydrogels' relative effectiveness. Citric acid-crosslinked banana stem cellulose hydrogel showed strong antibacterial activity with the largest inhibition zone (24 mm), outperforming cellulose (23 mm) and

eISSN Number: 3036-017X

carboxymethylcellulose (22 mm) hydrogels, indicating its enhanced antimicrobial potential (Fig. 18). Banana stem cellulose hydrogel with citric acid showed superior antibacterial activity, due to the cellulose's natural properties and citric acid's effects, like acidic pH and metal ion chelation, that inhibit bacterial growth.

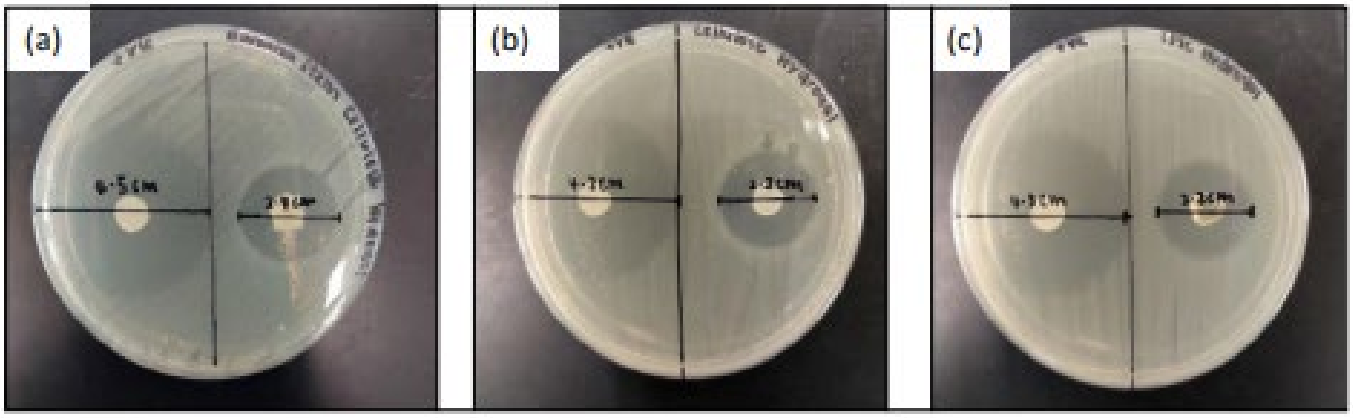

Fig. 18: Antibacterial assessment against *Escherichia coli* employing the disc diffusion method, encompassing (a) Banana Stem Cellulose (BSC) Hydrogel, (b) Cellulose Hydrogel, and (c) Carboxymethyl Cellulose (CMC) Hydrogel

3.4.4 Adsorption test

Fig. 20 shows a methylene blue standard curve with a strong linear relationship between absorbance and concentration (2–10 mg/L). The equation $y = 0.1488x$ ($R^2 = 0.9989$) indicates excellent linearity and precision. This allows accurate estimation of unknown dye concentrations during adsorption studies (Fig. 19). The data used to construct this curve are detailed in Table 1, which shows consistent absorbance values across three readings for each concentration, further validating the curve's reliability.

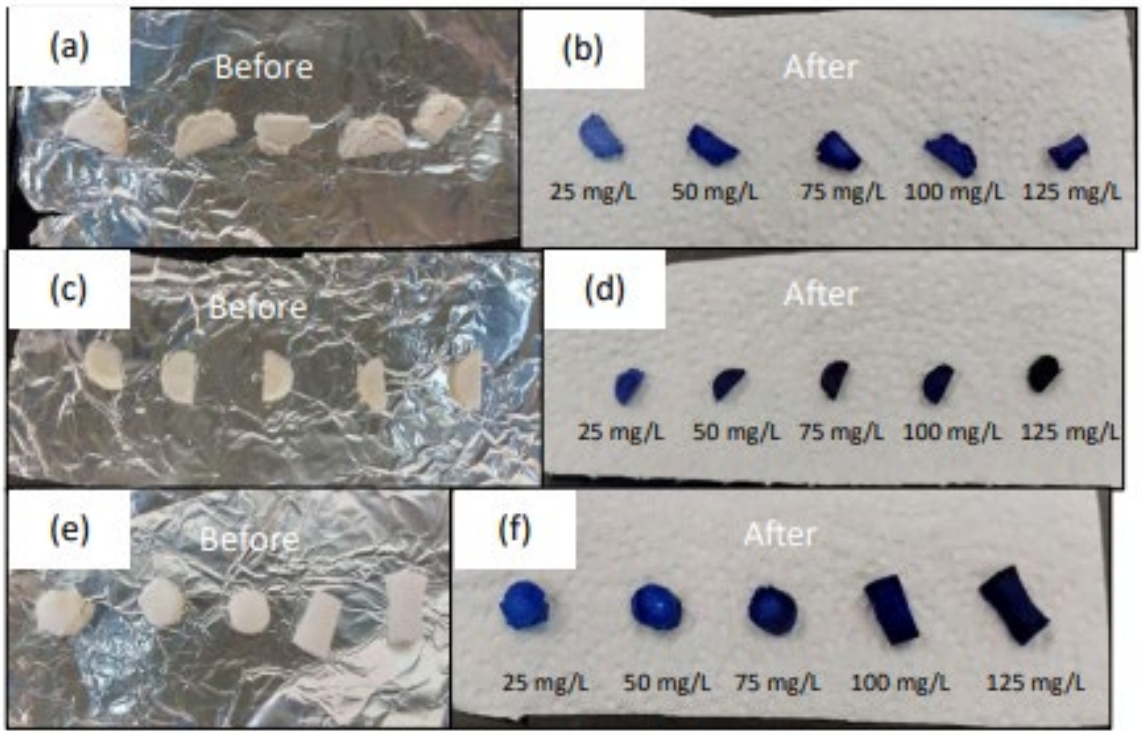

Fig. 19: Hydrogel before and after adsorption periods with methylene blue dye. The images show: (a) Banana Stem Cellulose Hydrogel before adsorption, (b) Banana Stem Cellulose Hydrogel after adsorption, (c) Cellulose Hydrogel before adsorption, (d) Cellulose Hydrogel post-adsorption, (e) Carboxymethylcellulose Hydrogel before adsorption, and (f) Carboxymethylcellulose Hydrogel after adsorption

eISSN Number: 3036-017X

Table 1: Measured density and moisture content of the manufactured wood composites

Concentration (mg/L)	Absorbance Reading 1	Absorbance Reading 2	Absorbance Reading 3	Average
2	0.274	0.278	0.288	0.280
4	0.659	0.648	0.644	0.650
6	0.915	0.925	0.908	0.916
8	1.189	1.198	1.203	1.197
10	1.445	1.455	1.449	1.450

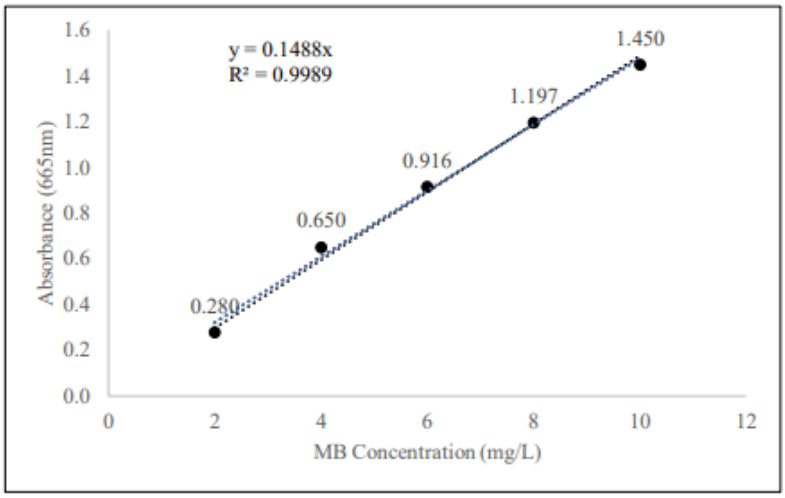

Fig. 20: Standard Curve for the Methylene Blue (MB)

Fig. 21 presents a bar graph comparing dye adsorption (Qe, mg/g) of Banana Stem Cellulose (blue), Cellulose (red), and Carboxymethylcellulose (green) hydrogels across concentrations of 25–125 mg/L. As shown in Table 2, Qe values for all three hydrogels increase with higher dye concentrations, highlighting their effectiveness in adsorption.

In the adsorption study, Banana Stem Cellulose Hydrogel adsorbed dye from 2.051 mg/g (25 mg/L) to 11.233 mg/g (125 mg/L), showing strong uptake. Cellulose Hydrogel showed similar results, increasing from 2.234 to 11.256 mg/g. Carboxymethylcellulose Hydrogel also performed well, rising from 2.261 to 11.608 mg/g. All hydrogels displayed a consistent increase in dye adsorption with concentration, as shown in Table 2 and Fig. 21.

Table 2: The amount of Dye Adsorbed for each concentration of the three types of hydrogel

Concentration (mg/L)	Dye Adsorb, Qe (mg/g)		
	Banana Stem Cellulose Hydrogel	Cellulose Hydrogel	Carboxymethylcellulose Hydrogel
25	2.051	2.234	2.261
50	4.013	4.406	4.505
75	6.478	6.818	6.900
100	8.772	8.978	9.238
125	11.233	11.256	11.608

eISSN Number: 3036-017X

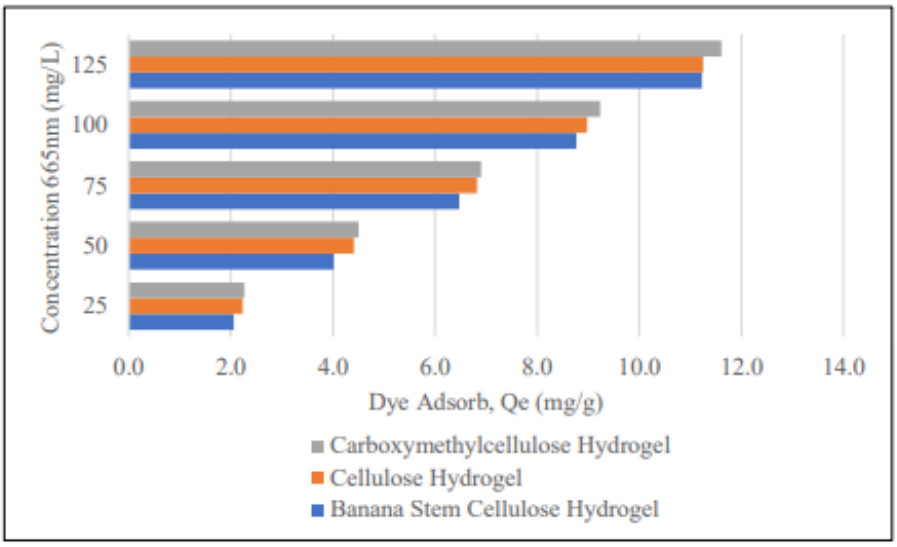

Fig. 21: Compare the quantitative bar graph depicting the dye adsorption capacity (Qe, mg/g) for three different types of hydrogels

The line graph in Fig. 22 shows dye adsorption capacities of Banana Stem Cellulose Hydrogel (BSC), Cellulose Hydrogel, and Carboxymethylcellulose (CMC) Hydrogel across concentrations of 25–125 mg/L. All hydrogels demonstrated a steady increase in adsorption. BSC Hydrogel rose from 2.051 to 11.233 mg/g, Cellulose Hydrogel from 2.234 to 11.256 mg/g, and CMC Hydrogel from 2.261 to 11.608 mg/g. These observed trends represent proportional and equivalent increases in dye adsorption capabilities over the concentration range for all three hydrogels.

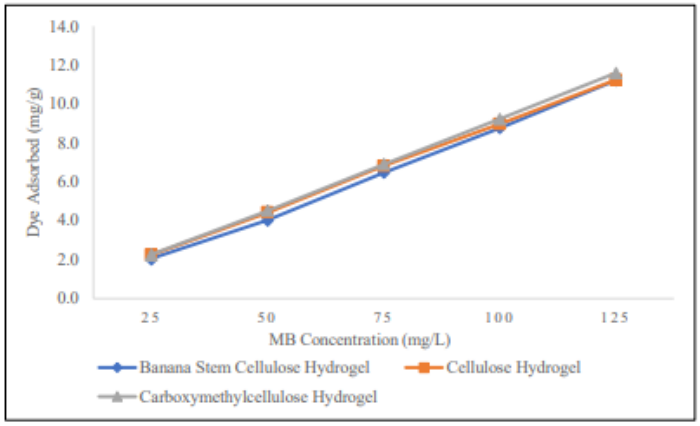

Fig. 22: Comparison Line graph of the treatments of dye adsorbed for three types of hydrogels

Fig. 23 illustrates the dye removal efficiency of three hydrogels across varying concentrations (25–125 mg/L). Banana Stem Cellulose Hydrogel shows fluctuating performance, starting at 81.19%, dipping slightly, then increasing to 89.72% at 125 mg/L. Cellulose Hydrogel maintains consistent efficiency, ranging from 88.47% to 89.90%. Carboxymethylcellulose Hydrogel shows a steady increase, from 89.59% to 92.70%, indicating improved performance with higher concentrations. In summary, the collective analysis unveils nuanced patterns in the removal percentages of these three hydrogels, offering valuable insights into their respective performances in dye removal across different concentration levels.

eISSN Number: 3036-017X

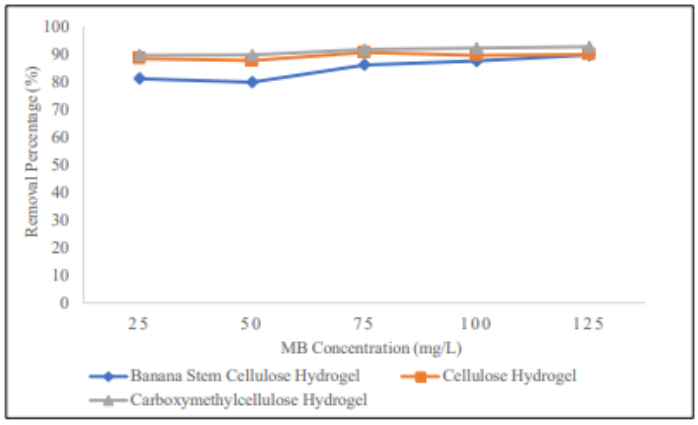

Fig. 23: Comparison line graph of the removal percentage for three types of hydrogels

3.4.5 Biodegradation test

The results come from a four-week study comparing the biodegradation effectiveness of Banana Stem Cellulose, Cellulose, and Carboxymethylcellulose Hydrogels. The study tracked weight loss over time to assess biodegradation stages. The following table and graph summarise the percentage weight loss for each hydrogel throughout the investigation.

Fig. 24 and Table 3 [1] show that CMC Hydrogel degrades fastest, with weight loss rising from 51% in week 1 to 100% by week 4. Banana Stem Cellulose and Cellulose Hydrogels degrade more slowly, starting at 40% and 51% in week 1, increasing to 91% and 89% respectively, by week 4. The Banana Stem Cellulose Hydrogel shows slightly better biodegradation than the Cellulose Hydrogel.

Initially, Cellulose Hydrogel degraded faster than Banana Stem Cellulose Hydrogel, but the trend reversed by the fourth week. The slower degradation of the cellulose-based hydrogels is attributed to their more crystalline and stable structure, with Banana Stem Cellulose also benefiting from natural components like hemicellulose and lignin. In contrast, the amorphous structure of CMC contributes to its reduced stability and faster breakdown.

Table 3: The quantification of biodegradation for each consecutive week

Type of Hydrogel	Initial Weight (g)	Biodegradation (g)				Weight loss (%)
		1st Week	2nd Week	3rd Week	4th Week	
Banana Stem Cellulose Hydrogel	1.175	0.704	0.529	0.469	0.106	91
Cellulose Hydrogel	1.073	0.522	0.377	0.307	0.115	89
Carboxymethylcellulose Hydrogel	1.867	0.914	0.400	0.199	-	100

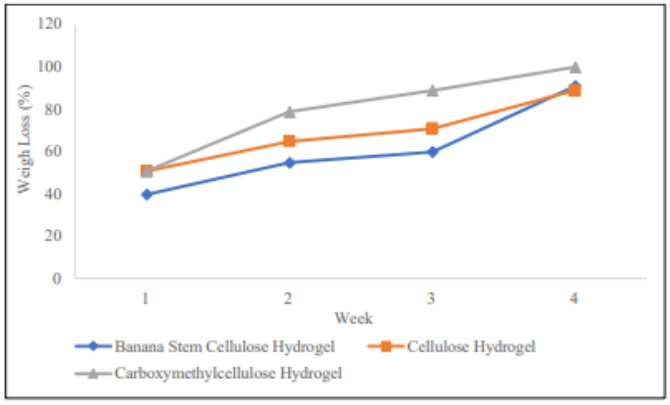

Fig. 24: Comparative line graph showcasing the weight loss during the biodegradation process for three different types of hydrogels

eISSN Number: 3036-017X

4. Conclusion

This study addresses wound dressing waste by pioneering sustainable hydrogels from banana stem cellulose and CMC, crosslinked with citric acid, offering an eco-friendly alternative with enhanced material properties. Using alkaline extraction, cellulose was eco-friendly sourced from banana byproducts, reducing waste. Citric acid crosslinking enhanced hydrogel properties for wound care. Characterisation showed promising biodegradation, antibacterial activity, and microstructure via SEM, including pore details. The hydrogels also demonstrated effective methylene blue adsorption, suggesting wastewater treatment potential. Overall, this research supports sustainable wound care and agricultural waste valorisation, offering insights for biomedical and environmental applications.

Acknowledgements

The authors express their sincere appreciation to the Faculty of Bioengineering and Technology, Universiti Malaysia Kelantan, Jeli Campus, for the financial support and facilities which made this study possible.

References

[1] Vijayaraghavan G, Dharan D, Sivamani S. Preparation of carboxymethyl cellulose from *Musa paradisiaca* pseudo stem using an alkaline treatment. Nat Environ Pollut Technol, 2022;21(5):2323-2327.

[2] Susi S, Ainuri M, Wagiman W, Falah M. Enhanced carboxymethyl cellulose based on empty fruit bunches in a high degree of substitution and thermal stability as a biocomposite film backbone. *Int J Chem Eng*, 2024;2024:3319401.

[3] Aridi AS, Ling CN, Ishak NA, Nor Nadiah MY, Ahmed MFM, Yusof YA. Structural FTIR analysis of cellulose functional groups isolated from *Leucaena leucocephala* pods using different bleaching agents. AgriRxiv, 2020;20203561010.

[4] Brahma R, Ray S. Optimization of extraction conditions for cellulose from jackfruit peel using RSM, its characterization and comparative studies to commercial cellulose. Meas Food, 2024;100130.

[5] Golor MM, Rosma D, Santoso SP, Soetaredjo FE, Yuliana M, Ismadji S, Ayucitra A. Citric acid-crosslinked cellulosic hydrogel from sugarcane bagasse: Preparation, characterization, and adsorption study. Chem Eng Trans, 2020;27:59-67.

[6] Li M, Qu H, Li Q, Lu S, Wu Y, Tang Z, Liu X, Yuan Z, Huang L, Chen L, Wu H. A carboxymethyl cellulose/chitosan-based hydrogel harvests robust adhesive, on-demand detachment and self-healing performances for deep burn healing. Chem Eng J, 2024;498:155552.

[7] Zhang W, Liu Y, Xuan Y, Zhang S. Synthesis and applications of carboxymethyl cellulose hydrogels. Gels, 2022;8(9):529.

[8] Shah TA, Zhihe L, Zhiyu L, Andong Z. Composition and role of lignin in biochemicals. In: Lignin - Chemistry, Structure, and Application. London: IntechOpen, 2022.

[9] Yuwono S, Wahyuningsih E, Noviany N, Kiswandono A, Simanjuntak W, Hadi S. Characterization of carboxymethyl cellulose (CMC) synthesized from microcellulose of cassava peel. Mater Plast, 2021;57(4):225-235.

[10] Al-Daas A, Azmi AS, Ali FB, Anuar H. The effect of alkaline treatment to pseudo-stem banana fibers on the performance of polylactic acid/banana fiber composite. J Nat Fibers, 2023;20(1):1-12.

[11] Bengtsson J, Peterson A, Idström A, de la Motte H, Jedvert K. Chemical recycling of a textile blend from polyester and viscose. Part II: Mechanism and reactivity during alkaline hydrolysis of textile polyester. Sustainability, 2022;14(11):6911.

eISSN Number: 3036-017X